Theoretical Study of $[N_3X]^+$ (X = O, S, Se, Te) Systems

Qian Shu Li* and Li Ping Cheng

School of Chemical Engineering and Materials Science, Beijing Institute of Technology, Beijing 100081, P. R. China

Received: January 13, 2003; In Final Form: May 6, 2003

A series of $[N_3X]^+$ (X = O, S, Se, Te) compounds have been examined with ab initio and density functional theory (DFT) methods. To our knowledge, these compounds, except for $[N_3O]^+$, are first reported here. The capped triangle structures are global minima for all singlet $[N_3X]^+$ systems. Several decomposition and isomerization pathways for the $[N_3X]^+$ species have been investigated. The capped triangle $[N_3X]^+$ structures are kinetically unstable, and they will easily dissociate into ground-state NX^+ and N_2 molecules. The pyramidal $[N_3X]^+$ species are likely to be stable because of their moderate dissociation or isomerization barriers (25.4−45.0 kcal/mol), and they may be regarded as suitable candidates for high energy-density materials (HEDMs) if they can be synthesized. The rhombus $[N_3S]^+$ is also likely to be stable, but the rhombus $[N_3Te]^+$ is not likely to be stable, and if it is formed in any process, it will transform into the pyramidal structure.

1. Introduction

There is currently a great deal of interest in the characterization and development of efficient and environmentally safe energy sources. Polynitrogen and nitrogen-rich compounds have been the subjects of intense and sustained theoretical and experimental studies[1−26] because of their potential use as HEDMs. Despite the fact that theory clearly indicates that many polynitrogen molecules such as N_4,[1−5] N_6,[1,6−8] and N_8,[1,9−11] are metastable, preparing and detecting them have posed a formidable challenge to experimentalists. Indeed, for many years, the only known pure nitrogen species were N_2 and N_3^-. It was not until 1999 that experimental evidence for the stable salts of the N_5^+ cation was reported.[12] But the recent observation of the N_4 molecule as a metastable species with a lifetime exceeding 1 μs,[13] together with the observation of a new but ill-characterized polynitrogen species from a discharge-generated nitrogen plasma[14] and the experimental detection of the long-sought pentazolate anion[15] indicates a bright future for experimental polynitrogen chemistry.

The isolation of stable salts of the N_5^+ cation[12] has put the spotlight on the search for other stable polynitrogen species. In recent years, besides pure polynitrogen molecules, the hypothetical existence of nitrogen-rich compounds has been the focus of many theoretical studies.[16−26] Zandwijk et al.[16] previously studied bipyramidal Li_2N_4 by using ab initio methods. Schleyer et al.[17] reported that the lithium salt, N_5Li, favors the planar C_{2v} structure containing dicoordinated lithium. Lein et al.[18] predicted the ferrocene-like Fe(η^5-N_5)$_2$ to be a strongly bonded complex with D_{5d} symmetry. Burke et al.[19] employed a theoretical characterization of the pentazole anion with metal counterions, where the counterions considered are Na^+, K^+, Mg^{2+}, Ca^{2+}, and Zn^{2+}. Straka[20] performed a theoretical study of the possibility of stabilizing the N_6 species as a planar hexagonal ring in M(η_6-N_6) (M = Ti, Zr, Hf, Th) systems. Gagliardi and Pyykk[21,22] have recently reported two new classes of compounds, Sc(η^7-N_7) and η^5-N_5^-−M -η^7−N_7^{3-} (M = Ti, Zr, Hf, and Th). They predicted that ScN_7 and N_5ThN_7 should have a fair chance of existing.

The above investigations focus mainly on the metal−polynitrogen compounds, and only a few studies[23−26] focus on polynitrogen−nonmetal compounds. But some NO clusters such as the smallest diatomic nitride oxide are also very energetic molecules. In fact, diatomic NO is known experimentally to be an explosive in the liquid state, with an enthalpy of about 21.6 kcal/mol relative to N_2 and O_2 products at 298 K.[23] Evangelisti[24] have also studied some NO clusters—N_2O_3, N_4O_6, and N_8O_{12}—with D_{3h}, T_d, and O_h symmetries, respectively, at SCF and MP2 levels of theory. He pointed out that these systems also show characteristics of HEDMs. Wilson et al.[25] have recently investigated the N_6O_n (n = 1−3) species, and the N_6O_3 system was found to be a completely planar D_{3h} system. To reinforce the notion that very high energy metastable forms of N_4 can exist, Engelke et al.[26] have employed an experimental and theoretical study of $[N_3O]^+$. They observed this cation via time-of-flight spectroscopy as a metastable species whose lifetime is at least 0.52 μs. To confirm the observed $[N_3O]^+$ with a chemically bound structure, they have made ab initio quantum chemical calculations. As a result, two possible chemically bound $[N_3O]^+$ structures were found, that is, the triplet C_s "linear" structure and the singlet C_{3v} pyramidal structure.[26] From an energy viewpoint, they predicted the C_s linear form to be the observed $[N_3O]^+$ in their experiments, but at the same time, they pointed out that energy considerations alone are not sufficient to decide this issue. Therefore, it is necessary to study $[N_3O]^+$ further and identify the isomers that are likely to be stable and to be observed experimentally.

In the present study, we will continue to study $[N_3O]^+$, and we expect to find new isomers. Because the atoms of O, S, Se, and Te are in the same column of the periodic table, their $[N_3X]^+$-type compounds should be similar in geometries and properties. Therefore, we also study $[N_3S]^+$ and $[N_3Se]^+$ as well as $[N_3Te]^+$ and attempt to find some stability rules for this series of compounds.

It should be noted that our work in the present study focuses only on the singlet $[N_3X]^+$ systems. Further study on the

* Corresponding author. E-mail: qsli@bit.edu.cn. Tel: +86-10-6891-2665. Fax: +86-10-6891-2665.

10.1021/jp034083s CCC: $25.00
Published on Web 06/20/2003

corresponding triplet systems is currently in progress and will be the subject of future publications.

2. Computational Methods

All calculations were performed using the Gaussian 98 program package.[27] We initially optimized geometries and calculated the harmonic vibrational frequencies for $[N_3X]^+$ (X = O, S, and Se) at the B3LYP/6-311+G* level of theory, where B3LYP is the DFT method using Becke's three-parameter nonlocal functional[28] with the nonlocal correlation of Lee, Yang, and Parr[29] and 6-311+G* is the split-valence triple-ζ plus polarization basis set augmented with diffuse functions.[30] Then, the geometries were refined, and the vibrational frequencies were calculated at the level of second-order Moller−Plesset perturbation theory (MP2)[31] with the 6-311+G* basis set. The $[N_3Te]^+$ system was optimized at the B3LYP and MP2 levels of theory, where the 6-311+G* basis set was used for nitrogen and the energy-adjusted Stuttgart ECPs were used on the heavier atom Te ($Z = 52$).[32,33] Stationary points were characterized as minima without any imaginary vibrational frequency and a first-order saddle point with only one imaginary vibrational frequency. For transition states, the minimum-energy pathways connecting the reactants and products were confirmed using the intrinsic reaction coordinate (IRC) method with the Gonzalez−Schlegel second-order algorithm.[34,35] Final energies were refined at the CCSD(T)[36]/6-311+G*//B3LYP/6-311+G* + ZPE (B3LYP/6-311+G*) level of theory. In addition to the structural and energetic investigations, the natural population and Wiberg bond indices (WBIs) analyses were also presented using the natural bond orbital procedure (NBO).[37,38]

3. Results and Discussion

The optimized structures for four $[N_3X]^+$ systems are illustrated in Figure 1. The total energies, zero-point energies (ZPE), relative energies (with ZPE corrections), and number of imaginary frequencies are tabulated in Table 1.

3.1. Geometric Structures and Energies of the $[N_3X]^+$ Species. We first performed ab initio calculations on a wide variety of singlet structures of $[N_3O]^+$ by using two different and sophisticated theoretical methods. As exhibited in Figure 1, besides the reported C_{3v} pyramidal structure (**1b**),[26] we have located two new structures, that is, the C_{2v} capped triangle (**1a**) and the C_s quasiplanar rhombus (**1c**) (in which the deviation from the planar rhombus structure is small, and the corresponding dihedral angle is about 30°). Furthermore, the capped triangle structure we located is the most energetically favored for all singlet $[N_3O]^+$ species considered here. For the heavier $[N_3X]^+$ species, we focused mainly on the three low-lying structures initially obtained for $[N_3O]^+$. As shown in Figure 1, we found that the capped triangle structures (**1a**−**4a**) are global minima for all four $[N_3X]^+$ systems. The pyramidal structures (**1b**−**4b**) are local minima for all $[N_3X]^+$ systems. The quasiplanar rhombus structures (**1c**−**3c**) are local minima for the $[N_3S]^+$ system and first-order saddle points for the $[N_3O]^+$ and $[N_3Se]^+$ systems. Regarding $[N_3Te]^+$, the quasiplanar rhombus structure (**4c**) is a local minimum at the B3LYP level of theory but a first-order saddle point at the MP2 level of theory. The C_{3v} pyramidal $[N_3O]^+$, $[N_3S]^+$, $[N_3Se]^+$, and $[N_3Te]^+$ structures are 57.0, 17.0, 12.2, and 13.7 kcal/mol higher in energy than their capped triangle structures at the B3LYP level of theory, respectively. But at the MP2 level, except for $[N_3O]^+$, their energies are very close to those of the capped triangle structures. The relative energies were found to be 5.5, 0.4, and 0.7 kcal/mol for X = S, Se, and Te, respectively. The corresponding value is 50.8 kcal/mol for the pyramidal $[N_3O]^+$. The C_s rhombus $[N_3X]^+$ isomers are energetically higher than their global minima by 49.8, 29.0, 21.7, and 20.0 kcal/mol at the B3LYP level of theory for X = O, S, Se, and Te, respectively.

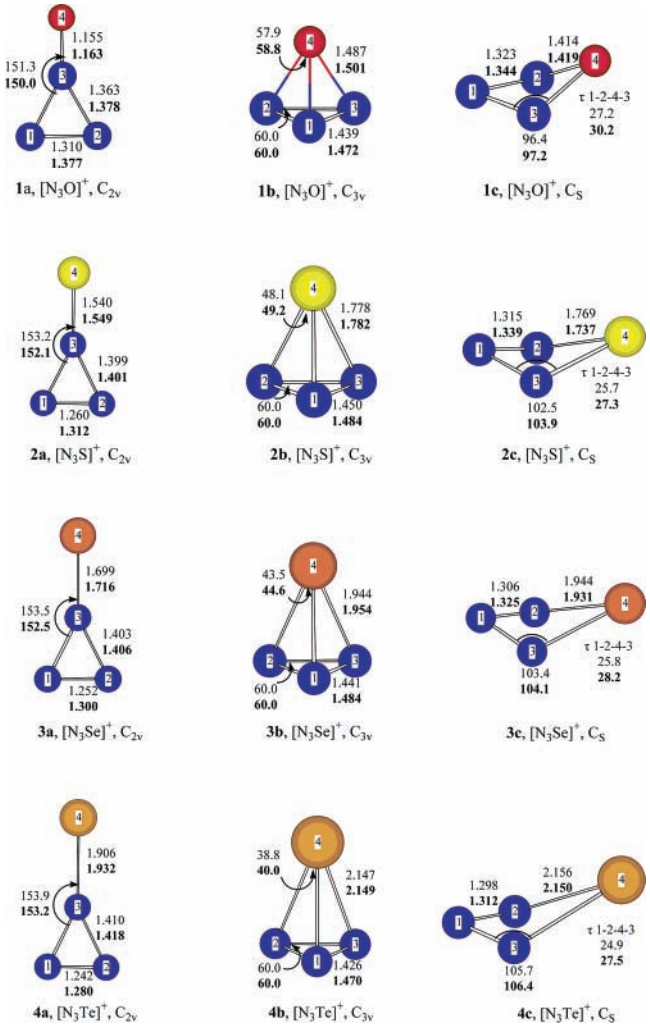

Figure 1. Optimized geometries (bond lengths in Å, bond angles in degrees) for $[N_3X]^+$ species at the B3LYP and MP2 (bold font) levels of theory.

TABLE 1: Total Energies (E),[a] Zero-Point Energies (ZPE),[b] and Relative Energies (RE)[c] for $[N_3X]^+$ Species

	B3LYP/6-311+G*			MP2/6-311+G*		
species	E[a]	ZPE[b]	RE[c]	E[a]	ZPE[b]	RE[c]
1a-$[N_3O^+]$ (C_{2v})	−238.93391	8.9 (0)	0.0	−238.38117	8.3 (0)	0.0
1b-$[N_3O]^+$ (C_{3v})	−238.84144	7.9 (0)	57.0	−238.29904	7.6 (0)	50.8
1c-$[N_3O]^+$ (C_s)	−238.85181	7.2 (1)	49.8	−238.28781	6.8 (1)	57.1
2a-$[N_3S]^+$ (C_{2v})	−561.97661	7.2 (0)	0.0	−561.03441	6.7 (0)	0.0
2b-$[N_3S]^+$ (C_{3v})	−561.94906	6.9 (0)	17.0	−561.02533	6.5 (0)	5.5
2c-$[N_3S]^+$ (C_s)	−561.92880	6.2 (0)	29.0	−560.98130	5.8 (0)	32.4
3a-$[N_3Se]^+$ (C_{2v})	−2565.32125	6.6 (0)	0.0	−2563.29777	6.2 (0)	0.0
3b-$[N_3Se]^+$ (C_{3v})	−2565.30139	6.3 (0)	12.2	−2563.29661	5.9 (0)	0.4
3c-$[N_3Se]^+$ (C_s)	−2565.28513	5.6 (1)	21.7	−2563.25454	5.3 (1)	26.2
4a-$[N_3Te]^+$ (C_{2v})[d]	−171.86589	6.3 (0)	0.0	−171.31817	5.9 (0)	0.0
4b-$[N_3Te]^+$ (C_{3v})[d]	−171.84358	6.0 (0)	13.7	−171.31747	6.2 (0)	0.7
4c-$[N_3Te]^+$ (C_s)[d]	−171.83265	5.4 (0)	20.0	−171.27642	5.2 (1)	25.5

[a] Total energies in hartrees. [b] Zero-point energies in kcal/mol. The integers in parentheses are the number of imaginary frequencies (NIMAG). [c] Relative energies with ZPE corrections in kcal/mol. [d] The 6-311+G* basis set was used for nitrogen, and energy-adjusted Stuttgart ECPs were used for Te.

TABLE 2: Energies (kcal/mol) of $[N_3X]^+$ Relative to Those of $N_2 + NX^+$

species	B3LYP/6-311+G*	MP2/6-311+G*	CCSD(T)/6-311+G*//B3LYP/6-311+G*
1a-$[N_3O]^+$ (C_{2v})	126.3	145.8	141.8
1b-$[N_3O]^+$ (C_{3v})	183.3	196.6	192.1
1c-$[N_3O]^+$ (C_s)	176.1	202.9	187.4
2a-$[N_3S]^+$ (C_{2v})	96.4	119.3	110.8
2b-$[N_3S]^+$ (C_{3v})	113.4	124.8	122.8
2c-$[N_3S]^+$ (C_s)	125.4	151.7	137.2
3a-$[N_3Se]^+$ (C_{2v})	86.2	113.0	99.9
3b-$[N_3Se]^+$ (C_{3v})	98.4	113.5	109.1
3c-$[N_3Se]^+$ (C_s)	107.9	139.3	120.6
4a-$[N_3Te]^+$ (C_{2v})[a]	67.7	106.5	83.7
4b-$[N_3Te]^+$ (C_{3v})[a]	81.4	107.2	91.2
4c-$[N_3Te]^+$ (C_s)[a]	87.7	132.0	103.4

[a] The 6-311+G* basis set was used for nitrogen, and energy-adjusted Stuttgart ECPs were used for Te.

The corresponding values at the MP2 level are 57.1, 32.4, 26.2, and 25.5 kcal/mol, respectively.

As shown in Figure 1, for each set of the similar structural $[N_3X]^+$ species, the heavier the X atom is, the longer the X−N distances are. The covalent radius for nitrogen is 0.70,[39] and the corresponding values for O, S, Se, and Te are 0.66, 1.04, 1.17, and 1.37,[39] respectively. Obviously, the X−N bond distances in the capped triangle structures are shorter than the sum of the covalent radii of the corresponding X atoms and nitrogen, and the X−N bond distances in the pyramidal and rhombus structures are longer than the sum of the covalent radii of the corresponding X atoms and nitrogen. In terms of NBO analysis, along group 6, going from O to Se, the calculated WBIs of X4−N3 in the capped triangle structures (**1a**−**3a**) range from 1.5 to 1.9, which are between the standard values of a single bond (1.0) and a double bond (2.0). But for the capped triangle $[N_3Te]^+$ (**4a**), the WBI of Te4−N3 is close to zero. Furthermore, all positive charges populate the Te atom evaluated by natural population analysis. Therefore, we predict that electrostatic interaction is dominant in this compound. However, in the pyramidal structures (**1b**−**4b**), going from O to Te, the WBIs of X4−N1 (N2 or N3) ranging from 0.9 to 1.0 are very close to that of the single bond (1.0). The corresponding values (0.8−1.0) in the rhombus structures (**1c**−**4c**) are also close to that of the single bond (1.0). Therefore, the X−N bond distances in the capped triangle structures should be shorter than those in the pyramidal and rhombus structures. Natural population analysis also shows that positive charges mainly populate the S, Se, and Te atoms for the $[N_3S]^+$, $[N_3Se]^+$, and $[N_3Te]^+$ systems, respectively, whereas for the $[N_3O]^+$ system things are different. Positive charges reside mainly on the N atoms adjacent to the O atom for all three singlet $[N_3O]^+$ isomers. This trend can be rationalized with the strong electronegativity of the oxygen atom.

The energy differences relative to $NX^+ + N_2$ molecules are listed in Table 2, and it appears that all $[N_3X]^+$ species would be very energetic materials. Furthermore, for each set of the similar structural $[N_3X]^+$ species, the heavier the X atom is, the lower the dissociation energy is. Therefore, it seems more reasonable to regard the smaller $[N_3X]^+$ molecules as suitable candidates for HEDMs.

3.2. Transition Structures and Reaction Barriers for Decomposition and Isomerization Reactions. To be viable as useful fuels, materials must be stable enough to be synthesized and stored without isomerization or decomposition. In other words, the energy barriers that prevent their decomposition and isomerization must be sufficiently high to provide stability. Generally, it is desirable to have all such barriers higher than 20 kcal/mol and preferably higher than 30 kcal/mol.[11] Therefore, it is very valuable to search all possible dissociation and isomerization routes for any new fuel candidates.

In the present study, the decomposition and isomerization reactions for the $[N_3X]^+$ (X = O, S, Se, Te) systems were investigated at the B3LYP level of theory. The optimized geometric parameters for 14 transition states are illustrated in Figure 2. Their total energies, zero-point energies (ZPE), and lowest vibrational frequencies are listed in Table 3. The energy differences between the minima and their corresponding transition states are tabulated in Table 4.

3.2.1. Dissociation Channels. (a) Capped Triangle $[N_3X]^+$ (C_{2v}) → $NX^+ + N_2$. These dissociations proceed in a straightforward manner with simple bond fissions. The transition states **TS1a**, **TS2a**, **TS3a**, and **TS4a** were located on the potential energy surfaces (PES). As shown in Figure 2, we can note that, compared with the capped triangle structures, the two bond lengths of N1−N3 and N2−N3 in the transition states are stretched to eliminate the NX^+ cations, whereas those of N1−N2 are actually compressed and almost become the N≡N bond. The barriers for dissociation are 13.5, 8.8, 8.5, and 8.8 kcal/mol for X = O, S, Se, and Te at the B3LYP level of theory, respectively. Single-point calculations at the CCSD(T) level decrease these values to 13.3, 8.2, 7.9, and 8.0 kcal/mol, respectively. These reactions are thus expected to occur easily, and the capped triangle $[N_3X]^+$ species should not be regarded as suitable candidates for new fuels.

(b) Pyramidal $[N_3X]^+$ (C_{3v}) → $NX^+ + N_2$. In the process of the pyramidal $[N_3X]^+ \rightarrow NX^+ + N_2$ reaction, four transition states **TS1b1**, **TS2b1**, **TS3b1**, and **TS4b1** were found to lie about 28.5, 37.4, 28.8, and 26.0 kcal/mol above the pyramidal $[N_3O]^+$, $[N_3S]^+$, $[N_3Se]^+$, and $[N_3Te]^+$ species at the CCSD(T) level of theory, respectively. On the way to forming **TS1b1**, **TS2b1**, **TS3b1**, and **TS4b1**, with the N1−N2−X4 and N1−N3−X4 angles increasing, the bond distances of N1−X4, N2−X4, and N2−N3 increase, whereas the N1−N2 and N3−X4 bond distances decrease. Starting from **TS1b1**, **TS2b1**, **TS3b1**, and **TS4b1**, the IRC calculations directly lead to dissociation into NX^+ (X = O, S, Se, or Te) and N_2, respectively. The moderate dissociation barriers of the pyramidal $[N_3O]^+$, $[N_3S]^+$, $[N_3Se]^+$, and $[N_3Te]^+$ species suggest that they are likely to be stable and to be observed experimentally.

3.2.2. Isomerization Channels. Possible interconversions of the capped triangle and pyramidal $[N_3X]^+$ species have been investigated. For $[N_3O]^+$, the two conformers **1a** and **1b** interconvert through a transition structure **TS1ab** (C_s). Con-

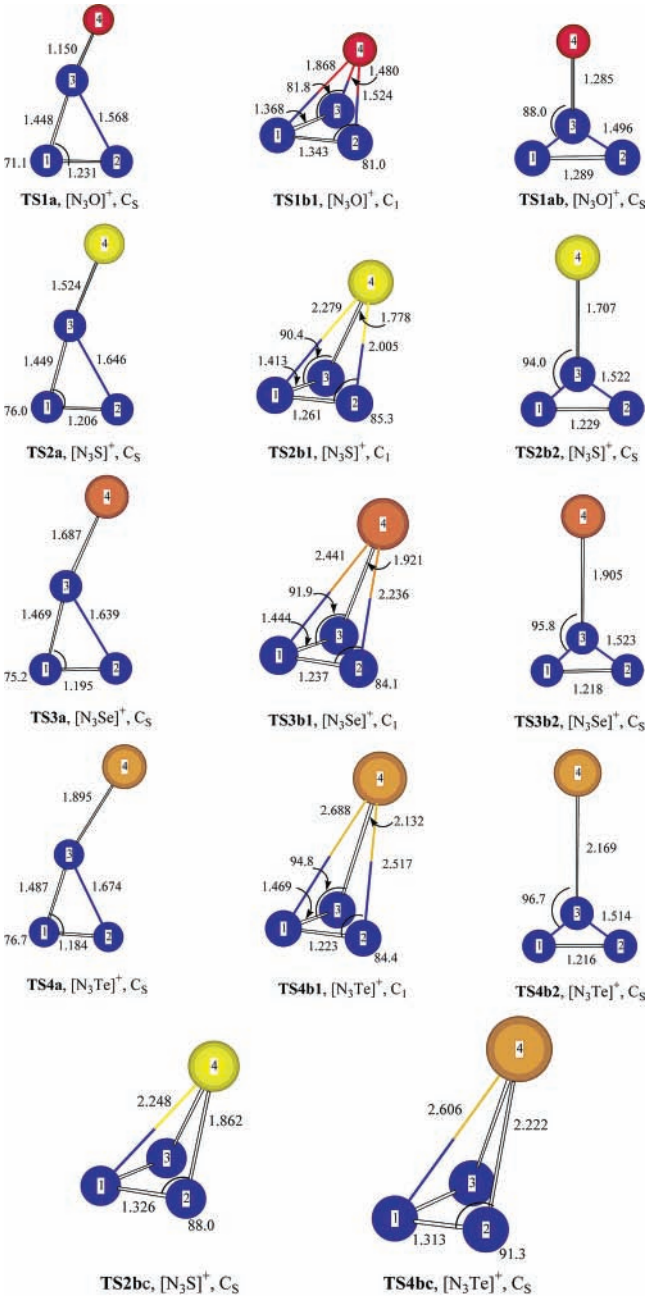

Figure 2. Fourteen transition states (bond lengths in Å, bond angles in degrees) for decomposition and isomerization reactions of $[N_3X]^+$ species.

former **1a** converts to **1b** with a barrier of 92.6 kcal/mol, and conformer **1b** converts to **1a** with a barrier of 42.3 kcal/mol. Such high barriers imply that both species **1a** and **1b** possess significant kinetic stability toward isomerization. We have also located three C_s-symmetric transition structures **TS2b2**, **TS3b2**, and **TS4b2** for $[N_3S]^+$, $[N_3Se]^+$, and $[N_3Te]^+$, respectively. As shown in Figure 2, the geometric structures of these transition states are very similar to that of **TS1ab**. However, starting from **TS2b2**, **TS3b2**, and **TS4b2**, the IRC calculations directly lead to dissociation into NX^+ (X = S, Se, or Te) and N_2, respectively. The barrier heights for decomposition reactions **2b** → **TS2b2** → $NS^+ + N_2$, **3b** → **TS3b2** → $NSe^+ + N_2$, and **4b** → **TS4b2** → $NTe^+ + N_2$ are respectively predicted to be 45.0, 27.6, and 25.6 kcal/mol at the CCSD(T) level of theory. Therefore, **TS2b2**, **TS3b2**, and **TS4b2** are virtually transition states for the decomposition of the pyramidal $[N_3X]^+$ (X = S, Se, and Te) structures, respectively. We have attempted to find possible transition states for the interconversions of the capped triangle and pyramidal $[N_3X]^+$ (X = S, Se, and Te) species, but IRC calculations confirmed that it is much more difficult to come back to the capped triangle structures than to dissociate into smaller molecules from the located transition states.

We have located one transition state **TS2bc** connecting the pyramidal $[N_3S]^+$(**2b**) to the rhombus $[N_3S]^+$ (**2c**). The typical bond distances and angles of **TS2bc** are reported in Figure 2.

TABLE 3: Total Energies (E), Zero-Point Energies (ZPE), and Lowest Vibrational Frequencies (υ_l) for the Transition States

	B3LYP/6-311+G*			
isomers	E (hartree)	ZPE (kcal/mol)	υ_l (cm^{-1})	CCSD(T)/6-311+G*//B3LYP/6-311+G*
TS1a (C_s)	−238.90969	7.2	1080i	−238.38541
TS1b1 (C_1)	−238.79520	5.9	1040i	−238.27899
TS1ab (C_s)	−238.77509	7.0	857i	−238.25874
TS2a (C_s)	−561.96047	5.9	755i	−561.06255
TS2b1 (C_1)	−561.89024	5.1	893i	−560.99557
TS2b2 (C_s)	−561.87739	5.9	731i	−560.98470
TS2bc (C_s)	−561.89110	5.2	929i	−560.99651
TS3a (C_s)	−2565.30571	5.3	714i	−2563.32396
TS3b1 (C_1)	−2565.25475	4.8	776i	−2563.27517
TS3b2 (C_s)	−2565.24646	5.5	616i	−2563.27823
TS4a (C_s)[a]	−171.84985	5.0	654i	−171.33271
TS4b1 (C_1)[a]	−171.80724	4.6	698i	−171.29145
TS4b2 (C_s)[a]	−171.80472	5.9	426i	−171.29423
TS4bc (C_s)[a]	−171.80808	4.6	692i	−171.29242

[a] The 6-311+G* basis set was used for nitrogen, and energy-adjusted Stuttgart ECPs were used for Te.

TABLE 4: Energy Differences (kcal/mol) of Transition States Relative to $[N_3X]^+$ Isomers (Including ZPE Corrections at the B3LYP/6-311+G* Level of Theory)

isomers	B3LYP/6-311+G*	CCSD(T)/6-311+G*// B3LYP/6-311+G*
1a (C_{2v})	0.0	0.0
TS1a (C_s)	13.5	13.3
TS1ab (C_s)	97.8	92.6
1b (C_{3v})	0.0	0.0
TS1b1 (C_1)	27.0	28.5
TS1ab (C_s)	40.7	42.3
2a (C_{2v})	0.0	0.0
TS2a (C_s)	8.8	8.2
2b (C_{3v})	0.0	0.0
TS2b1 (C_1)	35.1	37.4
TS2b2 (C_s)	44.0	45.0
TS2bc (C_s)	34.7	36.9
2c (C_s)	0.0	0.0
TS2bc (C_s)	22.7	22.5
3a (C_{2v})	0.0	0.0
TS3a (C_s)	8.5	7.9
3b (C_{3v})	0.0	0.0
TS3b1 (C_1)	27.8	28.8
TS3b2 (C_s)	33.7	27.6
4a (C_{2v})[a]	0.0	0.0
TS4a (C_s)[a]	8.8	8.0
4b (C_{3v})[a]	0.0	0.0
TS4b1 (C_1)[a]	21.4	26.0
TS4b2 (C_s)[a]	24.3	25.6
TS4bc (C_s)[a]	20.9	25.4
4c (C_s)[a]	0.0	0.0
TS4bc (C_s)[a]	14.6	13.2

[a] The 6-311+G* basis set was used for nitrogen, and energy-adjusted Stuttgart ECPs were used for Te.

In this transition structure, the bond distances of N1−S4, N2−S4, N3−S4, and N2−N3 increase on the way to forming **TS2bc**, whereas the N1−N2 and N1−N3 distances decrease. Both the N1−N2−S4 and N1−N3−S4 angles increase at the same time. The transition-state barrier on going from **2b** to **2c** is 36.9 kcal/mol, and from **2c** to **2b**, it is 22.5 kcal/mol at the CCSD(T)/6-311+G*//B3LYP/6-311+G* + ZPE (B3LYP/6-311+G*) level of theory. Thus, by comparison, the isomerization reaction between **2b** and **2c** is not easily carried out along this path. Similarly, we also found a transition state **TS4bc** connecting the pyramidal $[N_3Te]^+$ (**4b**) to the rhombus $[N_3Te]^+$ (**4c**). The transition-state barrier on going from **4b** to **4c** is 25.4 kcal/mol, and from **4c** to **4b**, it is 13.2 kcal/mol as evaluated by the single-point calculation. Therefore, the rhombus $[N_3Te]^+$ (**4c**) is not likely to be stable, and if it is formed in any process, it will transform into the pyramidal structure.

4. Summary

We examined a series of $[N_3X]^+$ (X = O, S, Se, Te) compounds in the present study. To our knowledge, these compounds, except for $[N_3O]^+$, are first reported here. Three singlet structures have been located for all $[N_3X]^+$ systems, that is, the C_{2v} capped triangle, the C_{3v} pyramidal, and the C_s quasiplanar rhombus structures. Among them, the capped triangle structures are global minima. For each set of the similar structural $[N_3X]^+$ species, the heavier the X atom is, the lower the dissociation energy is. Therefore, it seems more reasonable to regard the smaller $[N_3X]^+$ molecules as suitable candidates for HEDMs. Thermodynamically, except for the rhombus $[N_3O]^+$ and $[N_3Se]^+$, all known $[N_3X]^+$ species are local minima on their PESs at the B3LYP level of theory. However, the capped triangle structures are kinetically unstable, and the barriers for dissociation are only 13.3, 8.2, 7.9, and 8.0 kcal/mol for X = O, S, Se, and Te, respectively. But the pyramidal $[N_3X]^+$ species have the potential to be stable because of their moderate dissociation or isomerization barriers (25.4−45.0 kcal/mol). We have located two transition states **TS2bc** and **TS4bc** connecting the pyramidal $[N_3X]^+$ (X = S and Te), **2b** and **4b**, to the corresponding rhombus $[N_3X]^+$, **2c** and **4c**, respectively. The transition-state barrier on going from **2b** to **2c** is 36.9 kcal/mol, and from **2c** to **2b**, it is 22.5 kcal/mol. The corresponding barrier on going from **4b** to **4c** is 25.4 kcal/mol, and from **4c** to **4b**, it is 13.2 kcal/mol. This research suggests that the pyramidal $[N_3X]^+$ (X = O, S, Se, and Te) and the rhombus $[N_3S]^+$ species are likely to be stable and to be potential HEDMs if they can be synthesized.

References and Notes

(1) Glukhovtsev, M. N.; Jiao, H.; von Schleyer, P. R. *Inorg. Chem.* **1996**, *35*, 7124.
(2) Dunn, K. M.; Morokuma, K. *J. Chem. Phys.* **1995**, *102*, 4904.
(3) Frankel, M. M.; Chesick, J. P. *J. Phys. Chem.* **1990**, *94*, 526.
(4) Lee, T. J.; Rice, J. E. *J. Chem. Phys.* **1991**, *94*, 1215.
(5) Bittererov, M.; Brinck, T. *J. Phys. Chem. A* **2000**, *104*, 11999.
(6) Engelke, R. *J. Phys. Chem.* **1992**, *96*, 10789.
(7) Gagliardi, L.; Evangelisti, S.; Barone, V.; Roos, B. O. *Chem. Phys. Lett.* **2000**, *320*, 518.
(8) Tobita, M.; Bartlett, R. J. *J. Phys. Chem. A* **2001**, *105*, 4107.
(9) Leininger, M. L.; Sherrill, C. D.; Schaefer, H. F. *J. Phys. Chem.* **1995**, *99*, 2324.
(10) Tian, A.; Ding, F.; Zhang, L.; Xie, Y.; Schaefer, H. F. *J. Phys. Chem. A* **1997**, *101*, 1946.
(11) Chung, G.; Schmidt, M. W.; Gordon, M. S. *J. Phys. Chem. A* **2000**, *104*, 5647.
(12) Christe, K. O.; Wilson, W. W.; Sheehy, J. A.; Boatz, J. A. *Angew. Chem., Int. Ed.* **1999**, *38*, 2004.
(13) Cacace, F.; Petris, G.; Troiani, A. *Science* **2002**, *295*, 480.
(14) Zheng, J. P.; Waluk, J.; Spanget-Larsen, J.; Blake, D. M.; George Radziszewski, J. *Chem. Phys. Lett.* **2000**, *328*, 227.
(15) Vij, A.; Pavlovich, J. G.; Wilson, W. W.; Vij, V.; Christe, K. O. *Angew Chem., Int. Ed.* **2002**, *41*, 3051.
(16) Zandwijk, G. v.; Janssen, R. A. J.; Buck, H. M. *J. Am. Chem. Soc.* **1990**, *112*, 4155.
(17) Glukhovtsev, M. N.; Schleyer, P. von. R.; Maerker, C. *J. Phys. Chem.* **1993**, *97*, 8200.
(18) Lein, M.; Frunzke, J.; Timoshkin, A.; Frenking, G. *Chem.—Eur. J.* **2001**, *7*, 4155.
(19) Burke, L. A.; Butler, R. N.; Stephens, J. C. *J. Chem. Soc., Perkin Trans.* **2001**, *2*, 1679.
(20) Straka, M. *Chem. Phys. Lett.* **2002**, *358*, 531.
(21) Gagliardi, L.; Pyykk, P. *J. Am. Chem. Soc.* **2001**, *123*, 9700.
(22) Gagliardi, L.; Pyykk, P. *J. Phys. Chem. A* **2002**, *106*, 4690.
(23) Ramsay, J. B.; Chiles, W. C. In *Sixth Symposium (International) on Detonation*; Edwards, D. J., Ed.; Office of Naval Research, Department of the Navy: Arlington, VA, 1976.
(24) Evangelisti, S. *J. Phys. Chem. A* **1998**, *102*, 4925.
(25) Wilson, K. J.; Perera, S. A.; Bartlett, R. J.; Watts, J. D. *J. Phys. Chem. A* **2001**, *105*, 7693.
(26) Engelke, R.; Blais, N. C.; Sander, R. K. *J. Phys. Chem. A* **1999**, *103*, 5611.
(27) Frisch, M. J.; Trucks, G. W.; Schlegel, H. B.; Scuseria, G. E.; Robb, M. A.; Cheeseman, J. R.; Zakrzewski, V. G.; Montgomery, J. A., Jr.; Stratmann, R. E.; Burant, J. C.; Dapprich, S.; Millam, J. M.; Daniels, A. D.; Kudin, K. N.; Strain, M. C.; Farkas, O.; Tomasi, J.; Barone, V.; Cossi, M.; Cammi, R.; Mennucci, B.; Pomelli, C.; Adamo, C.; Clifford, S.; Ochterski, J.; Petersson, G. A.; Ayala, P. Y.; Cui, Q.; Morokuma, K.; Malick, D. K.; Rabuck, A. D.; Raghavachari, K.; Foresman, J. B.; Cioslowski, J.; Ortiz, J. V.; Stefanov, B. B.; Liu, G.; Liashenko, A.; Piskorz, P.; Komaromi, I.; Gomperts, R.; Martin, R. L.; Fox, D. J.; Keith, T.; Al-Laham, M. A.; Peng, C. Y.; Nanayakkara, A.; Gonzalez, C.; Challacombe, M.; Gill, P. M. W.; Johnson, B. G.; Chen, W.; Wong, M. W.; Andres, J. L.; Head-Gordon, M.; Replogle, E. S.; Pople, J. A. *Gaussian 98*, revision A.9; Gaussian, Inc.: Pittsburgh, PA, 1998.
(28) Becke, A. D. *J. Chem. Phys.* **1993**, *98*, 1372.
(29) Lee, C.; Yang, W.; Parr, R. G. *Phys. Rev. B* **1988**, *37*, 785.
(30) Hehre, W. J.; Radom, L.; Schleyer, P. v. R.; Pople, J. A. *Ab Initio Molecular Orbital Theory*; Wiley: New York, 1986.
(31) Møller, C.; Plesset, M. S. *Phys. Rev.* **1934**, *46*, 618.
(32) Andrae, D.; Haeussermann, U.; Dolg, M.; Stoll, H.; Preuss, H. *Theor. Chim. Acta* **1990**, *77*, 123.
(33) Fuentealba, P.; Preuss, H.; Stoll, H.; Szentpaly, L. v. *Chem. Phys. Lett.* **1982**, *89*, 418.
(34) Gonzalez, C.; Schlegel, H. B. *J. Chem. Phys.* **1989**, *90*, 2154.
(35) Gonzalez, C.; Schlegel, H. B. *J. Phys. Chem.* **1990**, *94*, 5523.
(36) Cizek, J. *Adv. Chem. Phys.* **1969**, *14*, 35.
(37) Carpenter, J. E.; Weinhold, F. *J. Mol. Struct.: THEOCHEM* **1988**, *169*, 41.
(38) Reed, A. E.; Weinstock, R. B.; Weinhold, F. *J. Chem. Phys.* **1985**, *83*, 735.
(39) http://chemed.chem.purdue.edu/genchem/topicreview/bp/ch7/size.html#cov.